Journal Pre-proof
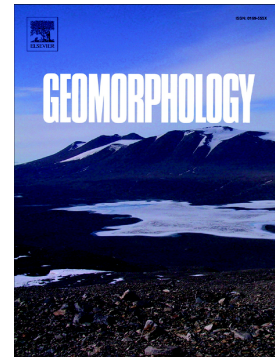
Landslide characteristics in the Loess Plateau, northern China

Yueren Xu, Mark B. Allen, Weiheng Zhang, Wenqiao Li, Honglin He

Please cite this article as: Y. Xu, M.B. Allen, W. Zhang, et al., Landslide characteristics in the Loess Plateau, northern China, *Geomorphology*(2020), https://doi.org/10.1016/j.geomorph.2020.107150

This is a PDF file of an article that has undergone enhancements after acceptance, such as the addition of a cover page and metadata, and formatting for readability, but it is not yet the definitive version of record. This version will undergo additional copyediting, typesetting and review before it is published in its final form, but we are providing this version to give early visibility of the article. Please note that, during the production process, errors may be discovered which could affect the content, and all legal disclaimers that apply to the journal pertain.

Landslide characteristics in the Loess Plateau, northern China

Yueren Xu[1, 2, *], Mark B. Allen[2], Weiheng Zhang[1], Wenqiao Li[1], Honglin He[3]

[1]Key Laboratory of Earthquake Prediction, Institute of Earthquake Forecasting, China Earthquake Administration, Beijing, China

[2]Department of Earth Sciences, Durham University, South Road, Durham, DH1 3LE, UK

[3]Key Laboratory of Active Tectonics and Volcano, Institute of Geology, China Earthquake Administration, Beijing, China

* Corresponding author at: Key Laboratory of Earthquake Prediction, Institute of Earthquake Forecasting, China Earthquake Administration, Beijing, China. E-mail address: yuefei189@gmail.com (Yueren Xu).

ABSTRACT

Landslides play an important role in landscape evolution of the Loess Plateau, northern China, but they have not been systematically analysed across the region. The contribution to regional rates of erosion and sediment budgets is poorly known as a consequence. Co-seismic landslides are a significant natural hazard, and exacerbate the threat posed by active faults in the region, but this aspect of the landslides is also poorly quantified. This paper presents inventories for ~80,000 landslides in the Loess Plateau, and analyses the distributions and extents. Four study areas focus on the epicentres of major (M >7) historical earthquakes, from AD 1303 (Hongdong), 1556 (Huaxian), 1718 (Tongwei) and 1920 (Haiyuan), which are likely to have been major triggers for landslides in these regions. A fifth study area focuses on landslides in the aftermath of localised storms in 2010 in the Tianshui region, to allow comparison of landslides clearly triggered by rainfall with landslides in the regional inventories. Landslides predominantly resulted from failure of the regional loess blanket that gives the region its name, or the soil profile developed above it. Rainfall-generated landslides

are dominantly surficial soil landslides. Landslides preserved in the four epicentral areas are larger and deeper, and resemble global bedrock landslides in the dimensions. Total volume of landslide in each of the four epicentral areas are on the order of 3-7 km^3; these volumes are likely to be the cumulative totals of repeated earthquakes in the same regions, with each event reactivating landslide scarps on hillsides. Comparison of landslide distributions and modern settlement patterns suggests that future M >7 earthquakes striking the Loess Plateau may trigger landslides that could directly hit 30-50% of the communities.

Key Words

Loess Plateau; Landslides; Co-seismic; Remote sensing interpretation

1. Introduction

This paper characterises landslides of the Loess Plateau, northern China, with the aim of understanding the distribution, size parameters, and the roles of earthquakes and rainfall in generating them. The Loess Plateau covers ~317,000 km^2, and results from loess deposition, mainly in Quaternary glacial periods (Liu et al., 1985; Derbyshire et al., 2000; Porter, 2001). Overall thicknesses of the loess deposits are typically >100 m, being thicker in the west and north (Fig. 1; Liu et al., 1985). The combination of climate and tectonics that produces the Loess Plateau created one of the most important landscapes on Earth for the development of human civilization (Rosen, 2008). Hillslopes have been terraced for greater agricultural production, and loess has been eroded and re-deposited in fault-controlled basins, occupied by the Yellow River (Huang He) and its tributaries, such as the Wei River (Fig. 1). Smaller tributaries are eroded into the loess, commonly creating a network of streams and rivers eroded into a low relief loess surface: the regional Loess Plateau is the

2

composite of these dissected surfaces. The valley slopes in this drainage network have higher topographic gradients than either the plateau surface or the valley floors (Li and Mo, 2019).

The Loess Plateau has suffered some of the deadliest earthquakes recorded globally (Table S1): events in AD 1303 (Hongdong), 1556 (Huaxian) and 1920 (Haiyuan) killed ~1.4 M people (Liu-Zeng et al., 2015; Liu et al., 2014). Other deadly earthquakes occurred in the historical record, including the 780 BC Qishan earthquake, which is one of the oldest events for which an historical record exists. Seismic risk, a function of fault activity and population density, (Stein and Liu, 2009), involves failure of the loess deposits in landslides. High death tolls occurred directly through loess landslides. Dwellings were built into, over, or at the base of loess slopes. The area is particularly distinctive for the habitations dug into loess slopes, known as yaodongs. These are especially prone to collapse during earthquakes and associated landslides. It is estimated >10,000 of the deaths in the 1920 earthquake were caused by landslides (Zhang and Wang, 1995; Derbyshire et al., 2000).

Despite this known association of major Loess Plateau earthquakes and landslides, the regional distributions and volumes of co-seismic loess landslides are unknown. One effect of this knowledge gap is that it is hard to calculate seismic risk for the Loess Plateau (Stein et al., 2012). Nor is the balance between tectonic uplift and erosion understood on earthquake cycle timescales (2000-3000 years; Xu et al., 2018). A global dimension is added to this problem, in that previous studies have focused on other terrains involving other substrates, with loess being under-represented (Larsen et al., 2010; Tanyas et al., 2017).

To address this knowledge gap, we studied landslides in the regions of the three most deadly earthquakes of the Loess Plateau, and also the thrust-related Tongwei earthquake (AD 1718) (State Seismology Bureau, 1988; National Seismology Bureau, 2009). This coverage means potential causative earthquakes of normal, thrust and strike-slip fault slip senses are all included. Earthquake parameters are summarized in Table 1.

3

Table 1. Characteristics of major earthquakes in the Loess Plateau.

Date	Name	Magnitude	Type	Fatalities	Rupture (km)	Slip (m)
1303	Hongdong	7.2-7.6	Normal	270,000	≤95	≤5
1556	Huaxian	≤8	Normal	830,000	70	≤6
1718	Tongwei	7.5	Thrust	70,000	(blind)	?
1920	Haiyuan	7.8	Strike-slip	270,000	230	5-10

It is not possible to determine the ages of the landslides in these areas, and to associate individual landslides firmly to a causative earthquake, or indeed any other cause. Therefore, estimates of landslide volume for each area represent an upper bound for the volume of material generated by each of the historic earthquakes, and are more realistically an estimate for co-seismic erosion over more than one earthquake cycle. The database of landslides in historical earthquake regions does not cover smaller, shallower landslides that are not preserved, but, by comparison with recent earthquakes the proportion of such smaller landslides to the total landslide area is relatively small (Xu et al.,2014).

Rainfall-induced landslides from storms in August 2010 in the region southeast of Tianshui were also studied (Fig. 1); the size and shape characteristics are compared with the data from the earthquake regions. This storm allows comparison of landslides definitely triggered by rainfall with the four larger areas, where we suspect, but cannot show *a priori,* that earthquakes triggered many of the major landslides.

2. Regional background

4

The Ordos region of northern China is undergoing active extension, albeit slowly, at ~1-2 mm/yr (Middleton et al., 2017). The stable Ordos Block is surrounded by rifts on most sides; in the southwest an active fold-and-thrust belt exists in the Liupanshan, which is at the eastern end of the left-lateral Haiyuan Fault. This unusual tectonic configuration means that faults of all slip senses occur in a relatively small region, within the limits of loess deposition. The cause of the extensional faulting is debated, with possible drivers in both the India-Eurasia collision and the interactions of oceanic plates with the eastern side of the Eurasian continent (Xu and Ma, 1992; Yin, 2010). The Haiyuan Fault and associated thrusts are part of the deformation system in the northeastern Tibetan Plateau. Such major strike-slip faults have been associated with eastwards translation of Eurasian crust ("extrusion tectonics"; Tapponnier et al., 1982). Alternatively, they represent the strike-slip component of strain partitioning, during oblique convergence across pre-existing, pre-collisional fault systems (Allen et al., 2017).

The AD 1303 Hongdong earthquake took place on the Huoshan Piedmont Fault (Xu et al., 2018). Although previously regarded as an M ~8 earthquake, partly on the basis of the ~270,000 death toll (Wang, 2003), scarp parameters such as length (~95 km) and maximum co-seismic slip (~5 m) are more consistent with a lower magnitude in the order of M_w 7.2-7.6 (Xu et al., 2018). The earthquake was a normal, dip-slip, event, which took place on the eastern side of the Shanxi Graben System, in the region between the Linfen and Taiyuan basins (Fig. 1b). For reasons that are unclear, the hangingwall to the Huoshan Piedmont Fault is a relative high between these two basins, rather than a depocentre. Loess is distributed on the hillslopes of this region, below the highest peaks and on either side of the fluvial deposits in the valley floors.

The AD 1556 Huaxian earthquake occurred on the south side of the Weihe Graben, with an epicentre along the western part of the Huashan Piedmont Fault (Fig. 1c). This fault system splays into three separate segments in the west, with the 1556 rupture taking place along the most northerly, basinward, segment (Fig. 1c). The event was reportedly the worst earthquake in history,

killing ~830,000 people, although this death toll was estimated by Kuo (1957) and seems to be recycled in the literature ever since, with little re-evaluation (Yuan and Feng, 2010). Likewise, although the magnitude is conventionally given as high as *M* 8.5, no evidence has been produced of a rupture on the scale of hundreds of kilometres that would be expected for an event of such a size. The observed surface rupture, of ~70 km (Rao et al., 2014), suggests an event on the scale of *M* ~7 (Wells and Coppersmith, 1994). Like the Huoshan area, the loess deposits near the Huashan Piedmont Fault lie on hillslopes, but at lower elevations than the most mountainous, bedrock terrain. The basinal areas of the Weihe Graben are filled by fluvial deposits of the Wei and Yellow rivers.

The AD 1718 Tongwei earthquake was not associated with a known regional surface rupture, or indeed any kind of exposed bedrock block (Fig. 1d). From the roughly NNW elongation of the isoseismal lines it is considered to have taken place on a fault with this orientation, representing a structure connected to the West Qinling Fault to the south (State Seismology Bureau, 1988; National Seismology Bureau, 2009). Magnitude is estimated as *M* 7.5 (State Seismological Bureau, 1988), but no regional surface rupture exists to measure and corroborate this value. The event is recorded as a thrust, but no clear evidence is found for the slip sense. This region is more continuously covered by loess deposits than the Huoshan or Huashan areas.

The *Mw* 7.8 Haiyuan earthquake of 26 December, AD 1920 caused ~230,000 deaths (Ren et al., 2016). The left-lateral Haiyuan Fault (HYF) formed a 230 km long surface rupture during this event, with a maximum coseismic displacement of 5 m (Fig. 1e). The affected region is at the western margin of the Loess Plateau. The relative youth of this event means that more eyewitness accounts are available for the extent of the devastation caused, including specific examples of landslides triggered by the earthquake (Close and McCormick, 1922; Zhuang et al., 2018).

The Tianshui region at the southwestern margin of the Loess Plateau was affected by severe storms over August 11-12 2010. Over 100 mm of rain fell during these two days in the worst-affected areas,

6

with one station recording 182 mm of rain in 24 hours and a peak rate of 96 mm in an hour (Wang et al., 2015). Whilst not on the scale of hurricane-strength storms, this is an unusual amount of rainfall for the Loess Plateau over such a period of time: total annual rainfall for this region is <500 mm. Forty-eight people were killed as a result of the floods and landslides.

3. Methods

3.1 Landslide mapping

Landslides were mapped manually and individually over a total area of >30,000 km^2 using high-resolution satellite imagery and field observations (Fig.1b-e, Fig.2, Tables S2-S5). We used Google Earth imagery to identify landslides. Manual mapping techniques were used to avoid the pitfalls of automated approaches, which include clustering of multiple events (Xu et al, 2016). Remote sensing observations were checked during 14 weeks of fieldwork by the authors, covering all regions in the study. Examples of larger-scale landslides on satellite imagery are shown in Fig. 2, with field photographs of different-scaled landslides in Fig. 3. We can provide data for the landslides in this study on request. Landslide data for each earthquake are available as a *.kml file and related *.xls file, including polygons for the outline of each earthquake-triggered landslide, and attributes i.e. length, width, height, area, top elevation, base elevation. The data will be shared via a link to an online database.

Historical records and reports were used to identify regions with landslides most likely to be created by the specific earthquakes in this study (Wang, 2003; Xu et al., 2018). An example of this analysis is shown for the Shanxi Graben in Fig. 4. The distribution of buildings that pre- or post-date the 1303 earthquake have been linked to monumental records, and used to construct isoseismals for this event (e.g. State Seismological Bureau, 1988), which can then be compared to the distribution of loess and bedrock (Fig. 4).

We compiled landslides for all four study areas, with three verification and cross-check stages, and measured attributes including length, width, and height. We did not attempt to record the smallest landslides (area <1,000 m^2) in these earthquake-affected regions, on the grounds that these landslides are likely to be short-lived in the landscape, and all extant examples will have formed long after the latest historic earthquake in each region. This approach is supported by our separate study of landslides generated during the 2010 storms in the Tianshui region (see below).

Results were cross-checked against previous local studies (Li et al., 2015; Sun et al., 2017; Zhuang et al., 2018). Our methodology was also applied to map co-seismic landslides of the 2008 Wenchuan earthquake (Fig. S1) where recent studies provide benchmarks (Li et al., 2014; Xu et al., 2016). Comparison of our data for the Wenchuan earthquake landslides with previous studies allows assessment of whether our methods and results are robust.

We analysed landslides generated by storms over August 10-11 2010 in the Tianshui region of the Ordos Plateau, for comparison with the earthquake-affected regions in our study. This area is located just to the east of the region struck by the 1718 Tongwei earthquake. Comparison of satellite imagery from before and after the storms permits the identification of landslides generated during or immediately after the rainfall that fell in the area during the storms.

3.2 Landslide volume

Loess Plateau landslides include examples where natural processes or human activity has cut through the landslide toe, allowing direct measurement of thickness of the landslides. We measured thickness in 18 landslides from the Hongdong and Huaxian regions in this way, and compared these data to headwall scarp heights (average of 3-5 measurements for each scarp), to establish an empirical relationship between the height of the headwall scarp and thickness of the landslide toe (Table S6). Scarp heights were measured from Google Earth digital elevation model (DEM) data for

232 landslides; the accuracy of this approach was cross-checked against 28 landslide scarps measured directly in the field by laser range finder, including the 18 where toe thickness was also measured directly (Table S6).

Empirical power law relationships were established between landslide volume and area using 50-66 sets of headwall scarp measurements for each of the four earthquakes in this study, in the standard form $V_{ls} = \sum_1^n \alpha A_i^\gamma$

where A_i is landslide area, V_{ls} is landslide volume, n is the number of landslides and the scaling parameters α and γ are constants that vary with setting. Landslide volumes were also calculated using previous global expressions of this power law (Guzzetti et al., 2009; Larsen et al., 2010).

3.3 Landslide strike rate

The risk posed by future landslides is obviously of importance to people living in the Loess Plateau. Our approach to assess the risk on a regional scale is to overlay the areas mapped as affected by landslides in each of our four earthquake-affected areas with modern settlement locations. The locations of these villages and towns were derived from the same satellite imagery used to identify and locate the landslides. The degree of overlap gives a first order idea of how landslide and settlement patterns interact. The rationale is that local practise is to re-build communities on the original sites after natural disasters: many places were destroyed by the historic earthquakes and landslides in this study, only to be re-built on the same site by survivors.

4. Results

Results of our analysis of the Wenchuan earthquake landslides are comparable with previous studies (Fig. S1), with our results being on the conservative side.

Landslides covering a total area of 1725 km^2 were mapped (Table 1) across our four study areas within the Loess Plateau with historic earthquakes. In all four cases a close association occurs between the concentrations of landslides and loess deposits, i.e. landslides are most common in the areas overlain by loess, rather than bedrock exposures at higher elevations or valley floors covered by fluvial deposits. Compare Fig. 1b and Fig. 4, for the Shanxi Graben System. Landslide frequency-area relationships are shown in Fig. 5; different fault types (thrust, normal, strike-slip) are not associated with different landslide-area distributions. Landslide dimensions are summarised on Fig. 6 for each region; these plots show that all four areas have landslides with similar characteristics, although the bulk of landslides in the Haiyuan area are shorter than the other areas. The average thickness of landslides in these areas is 9-14 m, which is higher than is normal for soil landslides (typically <3 m), but consistent with bedrock landslides.

Individual landslides are similar in each of the four earthquake-affected areas, in morphology and dimensions. Typically crescent-shaped headwall scarps occur at the top of river vallleys; these valleys are themselves commonly eroded into low relief loess plateau regions. Run-out zones down the valley slopes pass into accumulations of slipped material along the valley floors. Dammed lakes are common along the affected river valleys, especially in the Haiyuan region where the last major earthquake was only one hundred years ago. Some dammed lakes are silted up, especially in the regions where the last earthquake was older than at Haiyuan. No distinct differences occur in the appearance of the landslides between the four study areas: it is as easy to identify landslides close to the 1303 epicentre as the 1920 event. Landslide preservation is aided by the generation of numerous small surficial landslides on the scarps of older, larger, landslides; these minor landslides rejuvenate the larger scarps.

In the Hongdong region, five areas of concentrated landslides occur. Area A (11,950 landslides) is located in the hangingwall of the Huoshan Piedmont Fault, with ~73% of the total number of individual landslides for this region (Fig. 1b). Area A is a relative topographic high between the

10

Taiyuan and Linfen basins to the north and south. Landslides developed along tributary valleys of the Fen River drainage system. Areas B (701) and C (504) are at the north and south ends of the Huoshan Piedmont Fault, and close to the 1303 earthquake rupture. Intervening areas of higher ground are not covered by loess, and contain far fewer landslides. Areas D (2,139) and E (868) are further from the Huoshan Piedmont Fault, and so less likely to have been triggered by an earthquake along it, in AD 1303 or any other time. Areas D and E are excluded from further data analysis of this region, so that all of the landslides considered are likely to be associated with one causative fault, if not one earthquake. The Hongdong region lacks landslides on the scale of the very largest from the other three areas (Fig. 5).

The Huaxian region is associated with 6,767 mapped landslides. Two dense landslide areas are located at the western and eastern ends of the Huashan Piedmont Fault (Fig. 1c), in locations equivalent to clusters B and C at either end of the 1303 rupture (Fig. 1b). Other areas close to the 1556 earthquake contain fewer landslides: they tend to be underlain by either bedrock in the footwall uplift to the Huashan Piedmont Fault, or are in the alluvial plains of the Wei River (Fig. 1c).

We interpreted 5,019 landslides in the Tongwei region (Fig. 1d), concentrated between Tongwei and Gangu, north of the West Qinling Fault. The total landslide area is 635 km^2. As for the Hongdong and Huaxian regions, most landslides are within loess deposits, on the sides of river valleys that are themselves eroded into the relatively low relief plateau surface.

For the Haiyuan region, we interpreted 7,151 landslides (Fig. 1e), concentrated in seven areas on either side of the eastern segment of the Haiyuan Fault. The total landslide area is 277 km^2, which is smaller than the other three study areas.

Many landslide studies use published values for α and γ, or estimate thickness by the excavated volume. We establish empirical values for α and γ, using the volume-area relationships of the 232 landslides for which we have measured scarp heights (Fig. 7). The range of γ values (1.09-1.28) is

11

similar to soil-based landslides, but distinctly lower than bedrock landslides (typically ~1.4). Coefficients (α) are 0.49-2.45, higher than for either bedrock or soil-based landslides (0.074-0.273) (Larsen et al., 2010). Limits on the thickness of loess landslides are set by: i) basal contacts with underlying bedrock, and ii) moderate relief of fluvial valleys in Loess Plateau landscapes (typically 100s m compared with 1000s m at margins of the Tibetan Plateau). Both factors produce low γ values compared with bedrock landslides in mountain ranges. High α values are caused by the relative thickness of loess compared with soil. The five-fold difference in coefficient (α) between the four regions shows that landslide patterns were not identical. This variation may relate to the variable thickness of the thickness; late Pleistocene loess is thicker in the west than the east of the plateau. Thicker loess generates thicker landslides above the basal contact with bedrock or above stratigraphic boundaries within the loess itself.

Combining our estimates for parameters α and γ, with the areal extents of individual landslides (Fig. 6), we obtain total volume estimates for each set of landslides (Table 2), of ~3-7 km^3 (Fig. 8). Applying published scaling parameters produces greater volumes of landslides (Fig. 8; Table 2). If every landslide in each area was generated during the associated historical earthquake, these estimates of estimates would represent values of co-seismic mass-wasting. Given that an unknown proportion relate to older earthquakes or other causes, they must be regarded as maximum estimates. The estimated volumes can only account for landslides that have survived since the formation, which favours larger landslides. Small (<10^4 km^2) landslides, however, do not make a significant contribution to the total volume of landslides after recent earthquakes, such as the 2008 Wenchuan event (Fig. S1). Additionally, our analysis may underestimate contributions from rare, high volume landslides that cut into bedrock underlying the loess, where higher values of γ are appropriate; only one of the landslides in Fig. 2 has area >10^6 m^2.

12

Table 2. Landslide scaling relationships and estimates of volume.

Region	Relationship	α	γ	L_Area (km^2)	Volume (km^3)	Amap (km^2)	Mean erosion (m)
Hongdong	L1	0.146	1.332±0.005		2.91+0.17/-0.16		0.52
	L2	0.186	1.350±0.01		4.56+0.55/-0.49		0.81
	L3	0.257	1.36±0.01	488.71	7.07+0.86/-0.76	5,622	1.26
	G	0.074	1.450±0.009		5.70+0.62/-0.57		1.01
	This study	**0.4898**	**1.2752±0.01**		**5.15+0.62/-0.55**		**0.92**
Huaxian	L1	0.146	1.332±0.005		2.85+0.18/-0.18		1.14
	L2	0.186	1.350±0.01		4.53+0.60/-0.53	2,504	1.81
	L3	0.257	1.36±0.01	323.83	7.10+0.95/-0.84		2.84
	G	0.074	1.450±0.009		6.40+0.77/-0.69		2.56
	This study	**0.7363**	**1.2065±0.01**		**3.00+0.40/-0.35**		**1.20**
Tongwei	L1	0.146	1.332±0.005		6.74+0.46/-0.43		2.33
	L2	0.186	1.350±0.01		10.89+1.53/-1.34	2,889	3.77
	L3	0.257	1.36±0.01	635.00	17.16+2.42/-2.12		5.94
	G	0.074	1.450±0.009		16.30+6.74/-2.08		5.64
	This study	**2.4505**	**1.0865±0.01**		**4.68+0.64/-0.56**		**1.62**
Haiyuan	L1	0.146	1.332±0.005		2.07+0.13/-0.12		0.54
	L2	0.186	1.350±0.01		3.29+0.42/-0.38		0.85
	L3	0.257	1.36±0.01	277.86	5.13+0.66/-0.59	3,859	1.33
	G	0.074	1.450±0.009		4.44+0.52/-0.46		1.15
	This study	**0.9371**	**1.1655±0.01**		**1.81+0.23/0.20**		**0.47**

13

L1: global relationship for all landslides from Larsen et al (2010). G: global relationship for all landslides from Guzzetti et al (2009). L2: global relationship for all bedrock landslides from Larsen et al (2010). L3: global relationship for mixed bedrock and soil landslides in the Himalaya from Larsen et al (2010). Mean erosion represents the average lowering of the ground surface from landsliding and is calculated by dividing the estimated volume by the total study area (Amap).

Using our scaling parameters, we derive spatially-averaged denudations of 0.47-1.62 m for the landslide datasets. Like the total estimates of volume, these denudation values must be regarded as maximum estimates for each historic earthquake, and reduce with the (unknown) proportion of landslides that pre-date or post-date these events; they cannot at present be translated into Holocene rates of erosion.

4.1 2010 Tianshui storms

The region southeast of Tianshui was hit by storms over August 10-11, 2010 (Fig. 9). The affected region is crossed by the West Qinling Fault, and, to its south, the southern limit of loess deposits (Fig. 9). This means that the event is a test case for the effects of storms in generating landslides in the region, and provides an insight into the relative effects of severe rainfall on areas underlain by loess and pre-Quaternary bedrock. We mapped ~54,000 landslides in the region. These landslides are not visible in imagery from earlier in the same year, and so each landslide can confidently be matched to the 2010 storms (Fig. 10). Mapped landslides show two distinct peaks in the distribution curve for the lengths, corresponding to lengths of 100 m and 200 m (Fig. 11). Each peak represents >2 × 10^4 individual landslides. The average area of the landslides is 1,260 m^2, and the total area affected was 67.7 km^2.

No obvious correlation exists between the number of landslides or the size and the substrate, i.e. loess or bedrock (Fig. 9), although landslides were caused in the loess region north of the West Qinling Fault further away from the centre of the storm than for the bedrock regions south of this structure. Detailed measurements of the thickness have not been made, but the vast majority of

14

landslides generated in August 2010 appear to have been shallow, soil landslides, rather than events affecting the underlying loess or bedrock. It is notable how rapidly these landslides are disappearing from the landscape. The time sequence of satellite images from the affected area shows that the majority of bare slopes were at least partially re-vegetated within 10 years of the original event (Fig. 10). Not been enough time has elapsed for full tree cover to be established. Similar landslides are common across the Loess Plateau (Fig. 3), commonly located on the scarps of older, larger landslides. The ages of these landslides, however, are not commonly recorded: the 2010 Tianshui event represents an unusual circumstance where numerous small landslides can be related to a single meteorological cause.

4.2 Landslide strike rate

Roughly 30-50 % of modern settlements are located within the proximity of individual landslides mapped in the four historic earthquake zones (Figs. 1 and 12; Hongdong – 30%; Huaxian – 53%; Tongwei – 51%; Haiyuan 33%). This range emphasises the extent to which the inhabitants of the region are at risk from future landslides on the scale of the main historic earthquakes, in worst-affected areas, on scales of $>10^4$ km^2. The results have been derived from looking at simple overlaps; no detail exists on the extent to which settlements overlap with landslides, and of course it is not a precise predictive tool for estimating future impacts. Instances occur where the settlement is in the region of the landslide path, or has been (re)constructed over the piled-up material at the end of the landslide. Settlements are not built over the steep ground of landslide headwalls, but communities are commonly found at the lip of these scarps, such that they do not count in these percentages, but are at risk to future landslides in the same locality. Most of the settlements that overlap landslides are villages; towns tend to be concentrated in the larger river valleys, on terraces above the active river channel. No guarantee exists that these towns are beyond the limit of larger landslides: the

numerous landslide-dammed lakes in the region attest to the ability of some landslides to fill valleys below completely.

5. Discussion

The similarity of our analysis of Wenchuan landslides with previous studies (Fig. S1) gives confidence that our methods are robust, and that our identifications of Loess Plateau landslides are accurate. No Loess Plateau landslides occur on the scale of the very largest examples from Wenchuan (Dai et al., 2011; Yin et al., 2009; Xu et al., 2014, 2016), presumably because of limited local relief of <400 m, versus ≤3,000 m relief in the Wenchuan earthquake.

Of the four earthquake-affected study areas, only Haiyuan was affected by a major earthquake recent enough for numerous co-seismic landslides to have been documented, in records that are preserved (Close and McCormick, 1922). Even for this event no systematic mapping of new landslides occurred in the aftermath of the earthquake, and no comparison of pre- and post-earthquake landscapes. Therefore, it is impossible to know which landslide scarps were entirely new, and which scarps were reactivations of pre-existing features, originally generated in earlier events. For the other three areas even fewer direct observations exist about the age of the landslides in our surveys. It is likely that a high proportion of these landslides were active during and immediately after the historic earthquake in each area, but, like the 1920 Haiyuan event, we do not know which features were entirely new, and which represented reactivations of earlier landslide scarps.

Four of the areas worst-affected by loess landslides are at the ends of normal faults with historic ruptures, in the 1303 and 1556 earthquakes (Fig. 1). These areas are particularly vulnerable because they have low enough elevation and relief to have accumulated loess, but enough tectonically-generated relief exists to favour landslides. We highlight this particular combination of structure and landscape as having high co-seismic landslide risk.

16

The volume of landslides in the four earthquake areas are sizable, but we cannot convert the results into rates of erosion and sediment fluxes because we do not know the age range over which they formed. The volume estimates of 3-7 km^3 for the areas are comparable with volumes calculated for landslides in the 2008 Wenchuan earthquake (2.7–4.4 km^3; Li et al., 2014; Xu et al., 2016). It is an unlikely scenario that Loess Plateau volumes of landslides were as high as our estimates in each earthquake, given that an unknown proportion would have been generated by previous earthquakes, or at least resulted from reactivation of older landslide scarps. Our estimates represent an upper limit to co-seismic landslide volumes from each historic event.

Landslides generated during the 2010 Tianshui storms were small and surficial, and have limited potential for preservation in the landscape, as shown by the partial disappearance less than ten years after the event (Fig. 10). They are unlike the larger, deeper landslides that occur in each of the four regional inventories that we have compiled. In these latter areas, landslides have affected the loess layers below the soil horizon, and so resemble bedrock landslides worldwide.

At present no studies have provided regional age determinations – even relative ages - of the Loess Plateau landslides. The presence of landslides in regions last affected by a major earthquake hundreds of years ago suggests that they survive in the landscape for times equivalent to or longer than the seismic cycle in the region (2,000 – 3,000 years). Clear landslide scars occur in the region around the BC780 Qishan earthquake, at the western end of the Weihe Graben (Fig. 1a; Table S2), which is an indication of the durability of landslide scars in the loess landscape. In contrast, the rainfall-generated landslides that accompanied the 2010 Tianshui storms indicate how hillslopes can be modified in such weather events, but also how rapidly they recover.

We regard the Loess Plateau landscape as being shaped by many cycles of co-seismic landslides, modified by the semi-continuous action of rainfall-triggered events (Fig. 13). The preponderance of small, surficial landslides and absence of bedrock landslides generated during the 2010 Tianshui storms suggests that larger, deeper landslides in the landscape are primarily co-seismic in origin,

17

although no reason exists why other triggers are not possible. No doubt major earthquakes also generate numerous soil landslides, but these do not survive on the hundreds (thousands?) of years timescales recorded for the bedrock landslides.

The 30-50 % overlap of modern settlement locations with landslide extents highlights the danger to communities from future landslides (Fig. 1). This regional analysis provides no data about which individual settlements are most vulnerable in the event of future earthquakes, which is clearly an avenue for future research. Three aspects to the risk need highlighting, although these are qualitative points. First, many settlements are built at the lip of landslide scarps, where they are vulnerable to future landslides, despite not appearing in our analysis of overlaps. Second, if our conclusion that landslide scarps are commonly reactivated is correct, a settlement that has previously been struck by a landslide is not safe from future events. Third, distinct combination of features creates high risk areas: fluvially-dissected loess terrain near the ends of active fault scarps (Figs. 1b and 1c). Whilst all areas near faults and loess slopes are vulnerable, the devastating earthquakes of 1303 and 1556 point to these areas as having some of the higher risk from future co-seismic landslides.

6. Conclusions

We have performed a quantitative study of ~30,000 landslides of area $>10^4$ m^2 in the Loess Plateau, northern China, to characterise the nature and distributions. Our study has focused on four areas where major historic earthquakes occurred, which plausibly acted as triggers for landslides, although simple correlation cannot be proven. We have also documented ~50,000 landslides generated by storms in 2010 in the Tianshui region, to provide a case study of landslides clearly generated by rainfall, not seismic activity, in the same region.

The rainfall-generated landslides are smaller and surficial, and resemble soil landslides worldwide. Such landslides are present throughout the Loess Plateau, and are highly transient features in the landscape, based on the rapid disappearance after the 2010 event. In contrast, the larger landslides found elsewhere in the Loess Plateau are not represented in the 2010 inventory, and are present in concentrations near the epicentres of each of the major historic earthquakes, in regions covered by loess. We conclude that the great majority of these landslides are likely to be co-seismic, but cannot confirm whether they were initially generated in the latest major earthquake, or were reactivated at scarps produced during previous earthquakes. Although we have estimates of total volume for the loess landslides in each study area (3-7 km^3), it is not possible to convert these volumes into a robust estimate for each earthquake.

A 30-50% overlap exists between the location of modern settlements and areas affected by landslides, in the four main study areas. This result is a first order indication of the risk posed by future landslides to the regional population: we predict that future major earthquakes in these and equivalent areas will trigger loess landslides on a catastrophic scale.

Declaration of competing interest

The authors declare that they have no known competing financial interests or personal relationships that could have appeared to influence the work reported in this paper.

Acknowledgements

19

Appendix A. Supplementary data

Supplementary data to this article can be found online at Https:

Figure captions

Figure 1. Main historical earthquakes and active faults around the Loess Plateau, Northern China. **a,**

Distribution of major faults, basins and main earthquakes. Black dashed lines show boundary of the

Loess Plateau. Red lines denote main faults. Large red circles show the four main earthquakes

referred to in this study; white circles show other major earthquakes (Supplementary Table 1); white

boxes show earthquake date and recorded deaths. Small red circles show other earthquakes. Shanxi

Graben (SXG); Weihe Graben (WHG); Huoshan Piedmont Fault (HPF); Huashan Piedmont Fault

(HSPF); Haiyuan Fault (HYF); Tongwei Fault (TWF). Inset shows the location of **a** within Asia. **b,**

Distribution of landslides in the Hongdong region of the SXG. Black dashed line shows isoseimals for

the 1303 Hongdong earthquake (Min, 1995). Grey polygons show individual landslides. Thin red

dashed lines show main landslide areas. Red dots are modern settlements within main landslide

areas. **c**. Distribution of landslides in the Huaxian region. Black dashed line shows isoseimals for the

20

1556 Huaxian earthquake (Min, 1995). **d**. Distribution of landslides in the Tongwei region. Black dashed line shows isoseimal X for the 1718 Tongwei earthquake (Min, 1995). **e.** Distribution of landslides in the Haiyuan region. Black dashed line shows isoseimals for the 1920 Haiyuan earthquake (Min, 1995)

Figure 2. Examples of loess landslides in the Huaxian region, in Google Earth imagery. Located on Fig.1c

Figure 3. Field photographs of landslides in the Loess Plateau. Located on Fig.1. **a, b,** Examples of loess landslide scarps on different scales in the Tongwei region, including fresh, presumed rainfall-generated scarps, on the slopes of a major scarp. **c,** Loess landslide and associated dammed lake in the Haiyuan region. **d,** Example of a loess landslide in the Huaxian region. Baituyao is located on Fig. 2b.

Figure 4. Distribution of isoseismals of the 1303 earthquake and related records from historical literature and steles. Distribution of sediments, bedrock and loess in the southern Shanxi Graben. Black line shows isoseimals for the 1303 earthquake.

Figure 5. Relationships between landslide frequency and area. **a, b, c, d.** Except for the Hongdong region, the Loess Plateau inventories include landslides with area $>10^{6}$ m^{2}, especially the Tongwei region.

Figure 6. Dimensions of individual landslides mapped in this study. **a,** length **b,** width **c,** height.

Figure 7. Empirical landslide volume-area relationships, derived from landslides measured in each study area.

Figure 8. Estimates of landslide volume estimates, derived from this study, and from L1: global relationship for all landslides; L2: global relationship for all bedrock landslides; L3: relationship for

21

mixed bedrock and soil landslides in the Himalayas (Larsen et al., 2010); G: global relationship for all

landslides (Guzzetti et al., 2009).

Figure 9. Rainfall and landslide distribution map for the 2010 Tianshui storms. Yellow polygons

indicate rainfall-generated landslides.

Figure 10. Sequential satellite images (from Google Earth, ©Google 2020) for a region affected by

the 2010 Tianshui storms, located on Fig. 9. **a,** imagery pre-dating the storms. **b, c,** imagery

postdating the storms. Images centred on 34.2807^{o} N 105.8828^{o} E.

Figure 11. Frequency-area plot for landslides generated in the 2010 Tianshui storms.

Figure 12. Overlap of settlements and landslides in the vicinity of the 1718 Tongwei earthquake.

Grey polygons show individual landslides. Red dots are modern settlements within main landslide

areas.

Figure 13. Schematic cartoon for landslide development on the Loess Plateau. **a,** Larger landslides

are generated during earthquakes, and may dam the river valleys below the headwall scarps. **b**,

Larger landslide scarps become the preferential sites for later landslides that are rainfall-generated

(red patches). Dammed lakes fill over time.

Supplementary Figure

Figure S1. Comparison of analysis of landslides generated by the 2008 Wenchuan earthquake,

between our study and Xu et al (2014).

Supplementary Tables

22

Supplementary Table S1. List of historical and modern earthquakes in the Ordos area, between BC 780 and AD 1966.

Supplementary Table S2. List of 66 earthquake-triggered landslides used to derive the volume-area equation for the Hongdong landslide region.

Supplementary Table S3. List of 56 earthquake-triggered landslides used to derive the volume-area equation for the Huaxian landslide region.

Supplementary Table S4. List of 56 earthquake-triggered landslides used to derive the volume-area equation for the Tongwei landslide region.

Supplementary Table S5. List of 50 earthquake-triggered landslides used to derive the volume-area equation for the Haiyuan landslide region.

Supplementary Table S6. Field survey and DEM measurements of individual landslides used to calculate overall landslide thicknesses and volumes.

References

Allen, M.B., Walters, R.J., Song, S., Saville, C., De Paola, N., Ford, J., Hu, Z. and Sun, W., 2017,

Partitioning of oblique convergence coupled to the fault locking behavior of fold-and-thrust belts: Evidence from the Qilian Shan, northeastern Tibetan Plateau. Tectonics, 36, 1679-1698.

Close, U., and McCormick E., 1922, Where the mountains walked. National Geographic Magazine, 41, 445-464.

Dai, F.C., Xu, C., Yao, X., Xu, L., Tu, X.B. and Gong, Q.M., 2011, Spatial distribution of landslides triggered by the 2008 Ms 8.0 Wenchuan earthquake, China. Journal of Asian Earth Sciences, 40, 883-895.

Derbyshire, E., Wang, J. T., and Meng, X. M., 2000, A treacherous terrain: background to natural hazards in northern China, with special refrence to the history of landslides in Gansu Province, in Derbyshire, E., Meng, X. M., and Dijkstra, T. A., eds., Landslides in the Thick Loess Terrain of North-west China: Chichester, Wiley, 1-19.

Guzzetti, F., Ardizzone, F., Cardinali, M., Rossi, M., and Valigi, D., 2009, Landslide volumes and landslide mobilization rates in Umbria, central Italy. Earth and Planetary Science Letters, 279, 222-229.

Kuo, T.C. 1957, On the Shensi earthquake of January 23, 1556. Acta Geophysica Sinica, 6, 59-68.

Larsen, I. J., Montgomery, D. R., and Korup, O., 2010, Landslide erosion controlled by hillslope material. Nature Geoscience, 3, 247-251.

Li, G., West, A. J., Densmore, A. L., Jin, Z. D., Parker, R. N., and Hilton, R. G., 2014, Seismic mountain building: Landslides associated with the 2008 Wenchuan earthquake in the context of a generalized model for earthquake volume balance. Geochemistry Geophysics Geosystems, 15, 833-844.

Li, W., Huang, R., Pei, X., and Zhang, X., 2015, Historical Co-seismic Landslides Inventory and Analysis Using Google Earth: A Case Study of 1920 M8.5 Haiyuan Earthquake, China, Engineering Geology for Society and Territory, Vol 2: Landslide Processes, 709-712.

Li, Y. and Mo, P., 2019, A unified landslide classification system for loess slopes: A critical review. Geomorphology, 340, 67-83.

Liu-Zeng, J., Shao, Y. X., Klinger, Y., Xie, K. J., Yuan, D. Y., and Lei, Z. S., 2015, Variability in magnitude of paleoearthquakes revealed by trenching and historical records, along the Haiyuan Fault, China. Journal of Geophysical Research-Solid Earth, 120, 8304-8333.

Liu, D., 1985, Loess and Environment, Beijing, Chinese Science Publishing House (in Chinese).

Liu, M., Wang, H., Ye, J. Y., and Jia, C., 2014, Intraplate earthquakes in North China, in Talwani, P., ed., Intraplate Earthquakes: Cambridge, Cambridge University Press, 97-125.

Middleton, T.A., Parsons, B. and Walker, R.T., 2017, Comparison of seismic and geodetic strain rates at the margins of the Ordos Plateau, northern China. Geophysical Journal International, 212, 988-1009.

Min, Z., 1995, Catalogue of Historical strong earthquake in China. Beijing, Seismological Press (in Chinese),1-118.

National Seismology Bureau, 2009, Strong earthquake catalogue in historical China, Seismological Press.

Porter, S. C., 2001, Chinese loess record of monsoon climate during the last glacial-interglacial cycle. Earth-Science Reviews, 54, 115-128.

Rao, G., Lin, A. M., Yan, B., Jia, D., and Wu, X. J., 2014, Tectonic activity and structural features of active intracontinental normal faults in the Weihe Graben, central China: Tectonophysics, 636, 270-285.

Ren, Z., Zhang, Z., Chen, T., Yan, S., Yin, J., Zhang, P., Zheng, W., Zhang, H. and Li, C., 2016, Clustering of offsets on the Haiyuan fault and their relationship to paleoearthquakes. Geological Society of America Bulletin, 128, 3-18.

Rosen, A. M., 2008, The impact of environmental change and human land use on alluvial valleys in the Loess Plateau of China during the Middle Holocene. Geomorphology, 101, 298-307.

State Seismology Bureau, 1988, Research on active faults system around the Ordos block,

Seismological Press.

Stein, S., Geller, R. J., and Liu, M. A., 2012, Why earthquake hazard maps often fail and what to do about it. Tectonophysics, 562, 1-25.

Stein, S., and Liu, M., 2009, Long aftershock sequences within continents and implications for earthquake hazard assessment. Nature, 462, 87-89.

Sun, P., Li, R. J., Jiang, H., Igwe, O., and Shi, J. S., 2017, Earthquake-triggered landslides by the 1718 Tongwei earthquake in Gansu Province, northwest China. Bulletin of Engineering Geology and the Environment, 76, 1281-1295.

Tanyas, H., van Westen, C. J., Allstadt, K. E., Jessee, M. A. N., Gorum, T., Jibson, R. W., Godt, J. W., Sato, H. P., Schmitt, R. G., Marc, O., and Hovius, N., 2017, Presentation and Analysis of a Worldwide Database of Earthquake-Induced Landslide Inventories. Journal of Geophysical Research-Earth Surface, 122, 1991-2015.

Tapponnier, P., Peltzer, G., Le Dain, A.Y., Armijo, R. and Cobbold, P., 1982, Propagating extrusion tectonics in Asia: New insights from simple experiments with plasticine. Geology, 10, 611-616.

Wang R.D. 2003, Collection of earthquake monument in Shanxi Province. Taiyuan: Beiyue Literature and Art Press, 1-497 (in Chinese).

Wang X.L., Zhu Y.J., Li Y., 2015, Analysis of a heavy rainfall process in summer over Tianshui. Journal of Agriculture, 5, 59-64. (in Chinese with English Abstract).

Wells, D.L. and Coppersmith, K.J., 1994, New empirical relationships among magnitude, rupture length, rupture width, rupture area, and surface displacement. Bulletin of the Seismological Society of America, 84, 974-1002.

Xu, C., Xu, X., Yao, X., Dai F. 2014, Three (nearly) complete inventories of landslides triggered by the May 12, 2008 Wenchuan Mw 7.9 earthquake of China and their spatial distribution statistical analysis. Landslides, 11, 441–461. https://doi.org/10.1007/s10346-013-0404-6

Xu, C., Xu, X., Shen, L., Yao, Q., Tan, X., Kang, W., Ma, S., Wu, X., Cai, J., Gao, M., and Li, K., 2016, Optimized volume models of earthquake-triggered landslides. Scientific Reports, 6, 29797.

Xu, X. and Ma, X., 1992, Geodynamics of the Shanxi rift system, China. Tectonophysics, 208, 325-340.

Xu, Y. R., He, H. L., Deng, Q. D., Allen, M. B., Sun, H. Y., and Bi, L. S., 2018, The CE 1303 Hongdong earthquake and the Huoshan Piedmont Fault, Shanxi Graben: Implications for magnitude limits of normal fault earthquakes. Journal of Geophysical Research, 123, 3098-3121.

Yin, A., 2010, Cenozoic tectonic evolution of Asia: A preliminary synthesis. Tectonophysics, 488, 293-325.

Yin, Y., Wang, F. and Sun, P., 2009, Landslide hazards triggered by the 2008 Wenchuan earthquake, Sichuan, China. Landslides, 6, 139-152.

Yuan T.H. and Feng, X.J., 2010, The 1556 Great Huaxian Earthquake, Seismological Press, Beijing, 1-148.

Zhang, Z. and Wang, L., 1995, Geological disasters in loess areas during the 1920 Haiyuan Earthquake, China. GeoJournal, 2-3, 269-274.

Zhuang, J., Peng, J., Xu, C., Li, Z., Densmore, A., Milledge, D., Iqbal, J. and Cui, Y., 2018, Distribution and characteristics of loess landslides triggered by the 1920 Haiyuan Earthquake, Northwest of China. Geomorphology, 314,1-12.
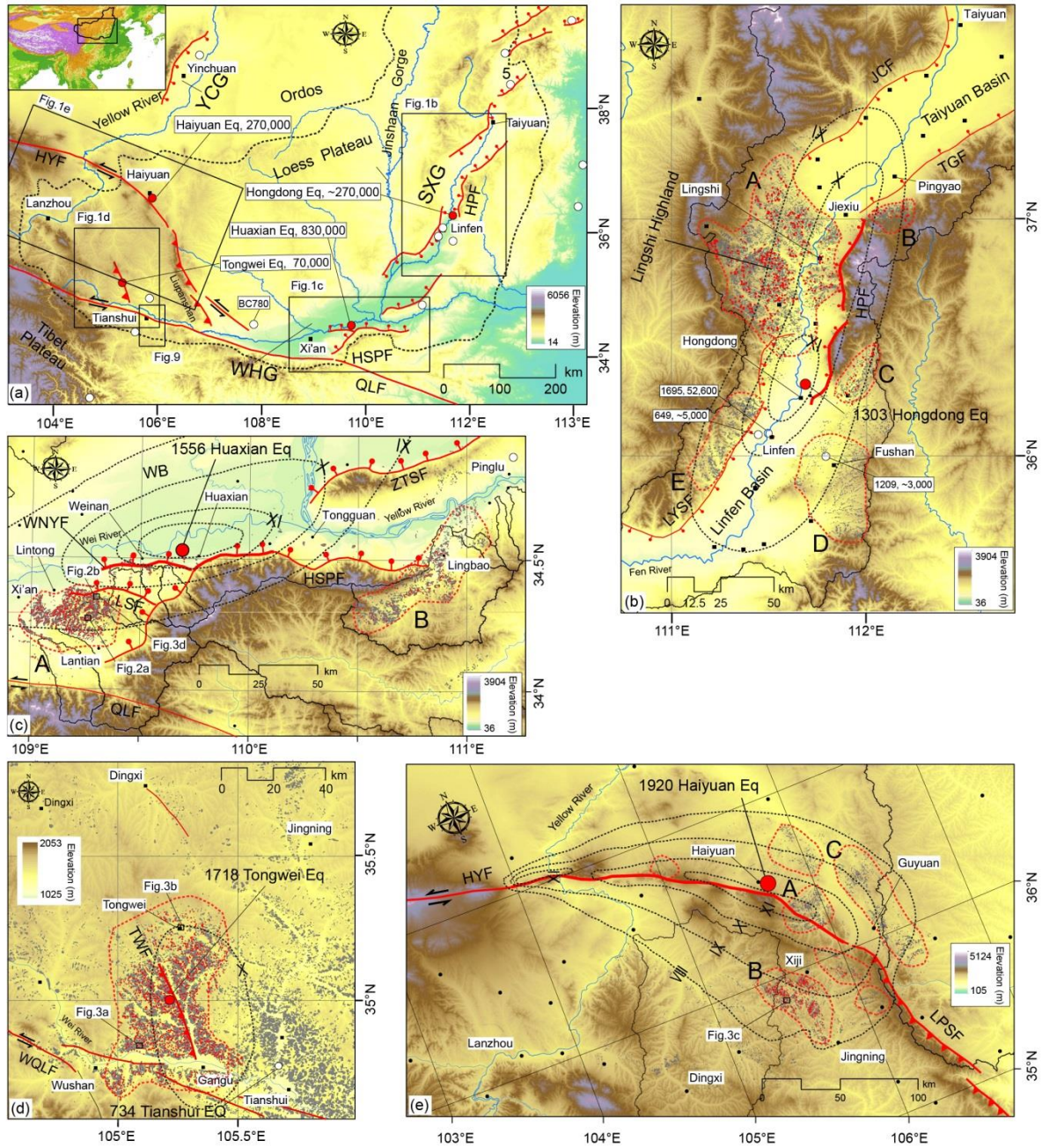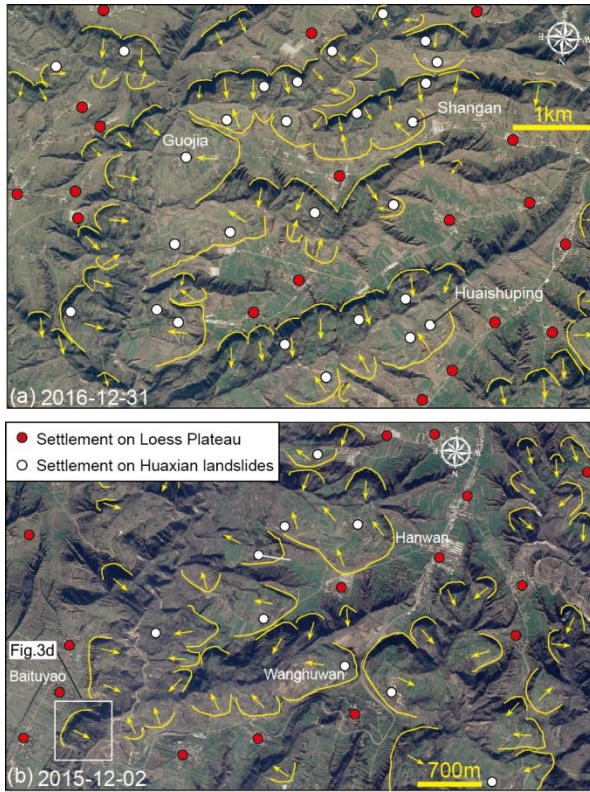
Fig.1

Fig.2
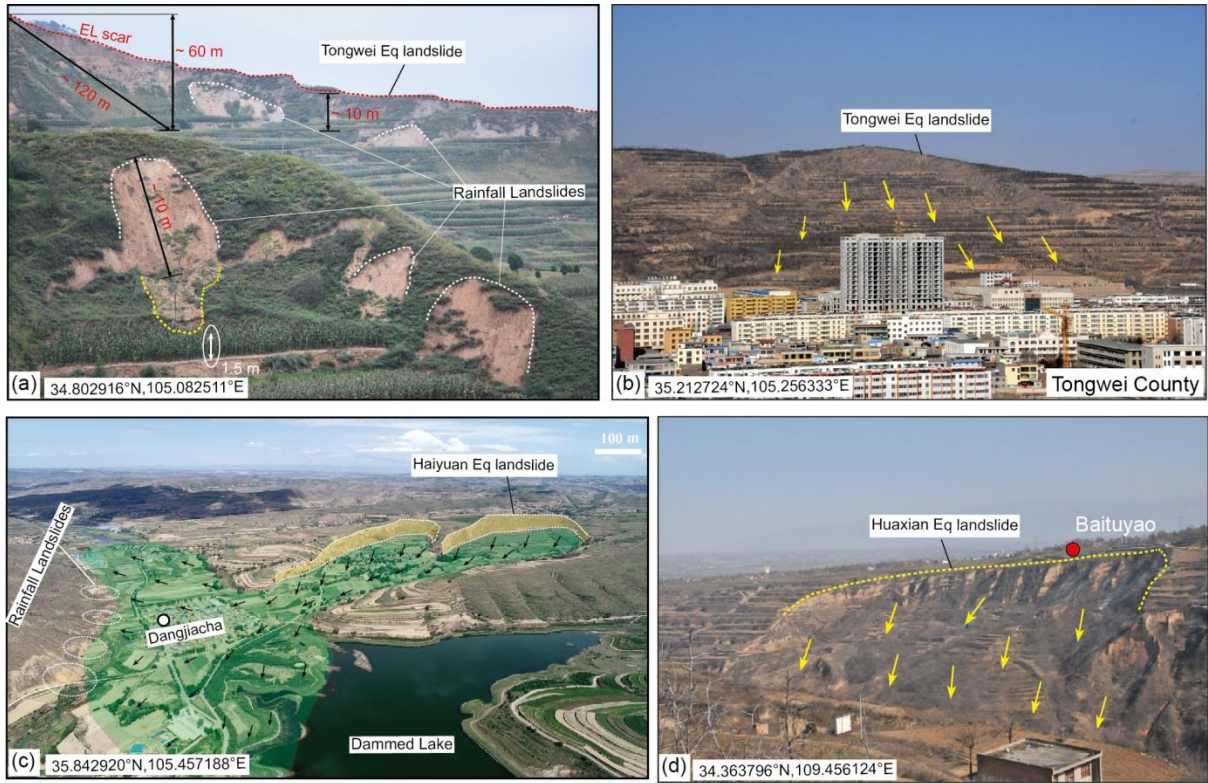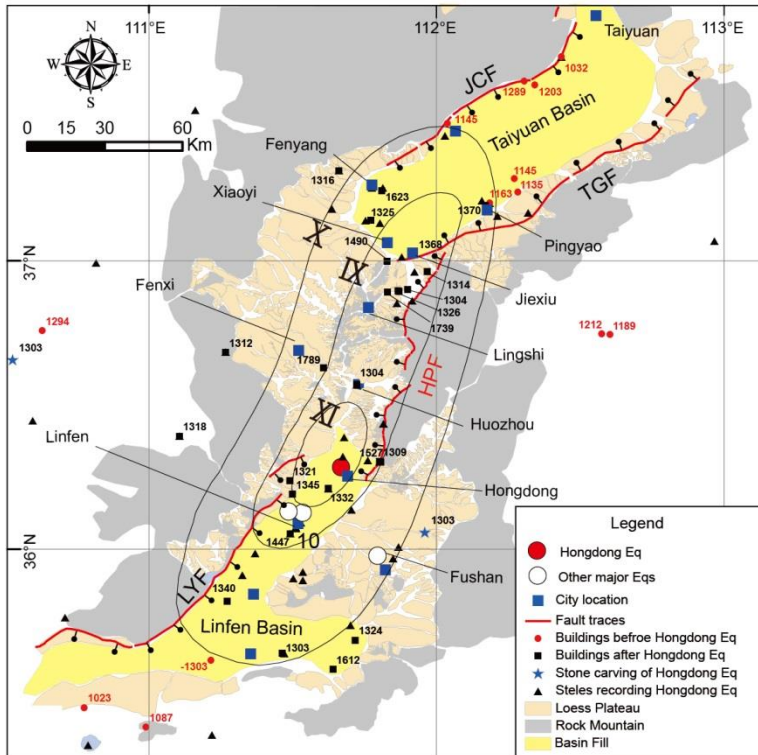
Fig.3

Fig.4

Fig.5
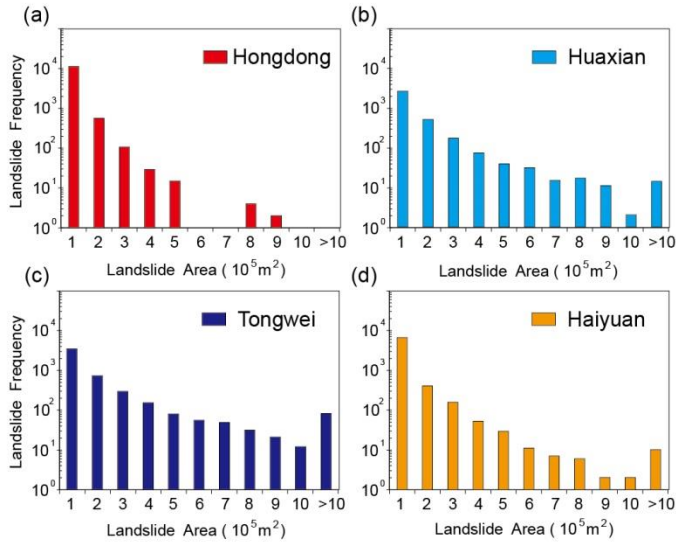
Fig.6
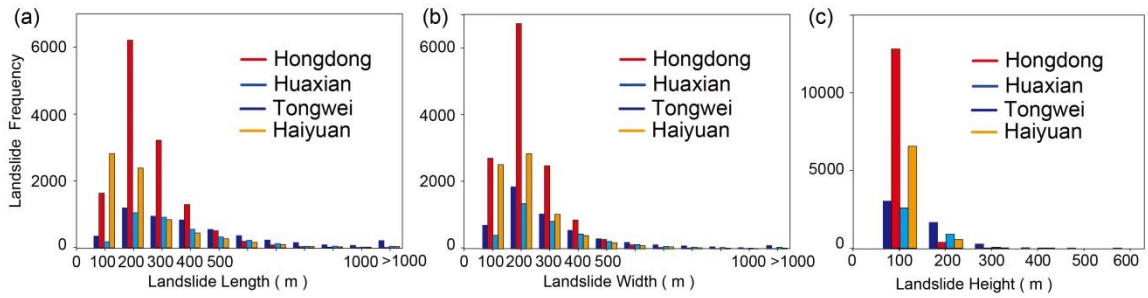
Fig.7
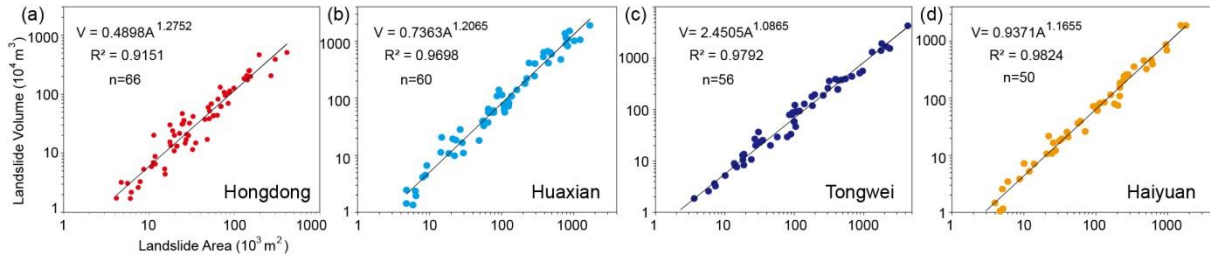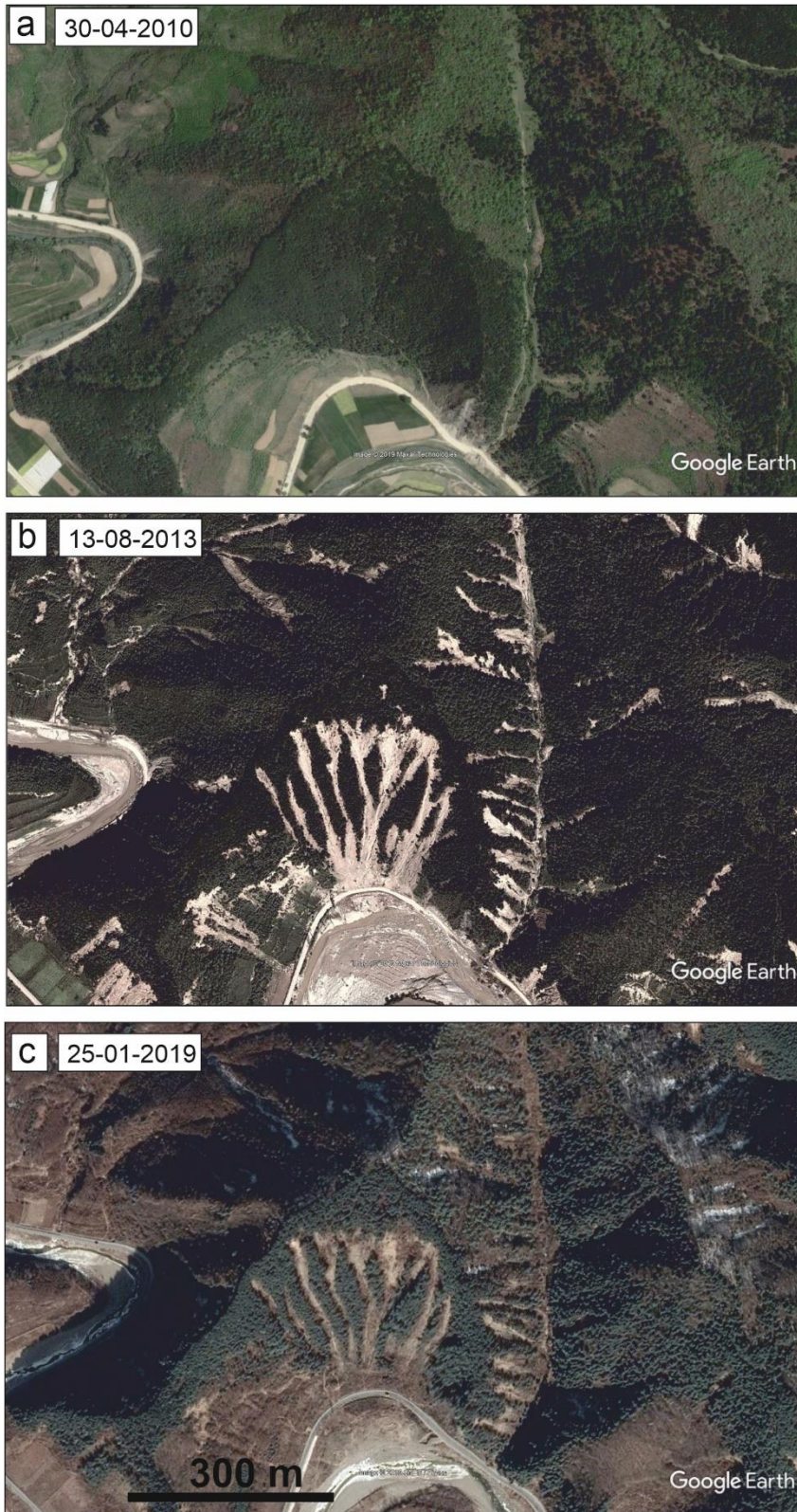
Fig.8
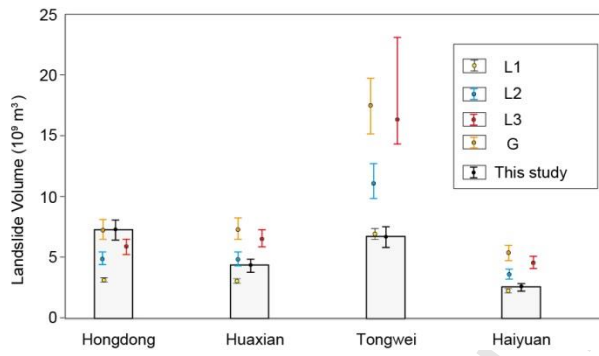
Fig.9
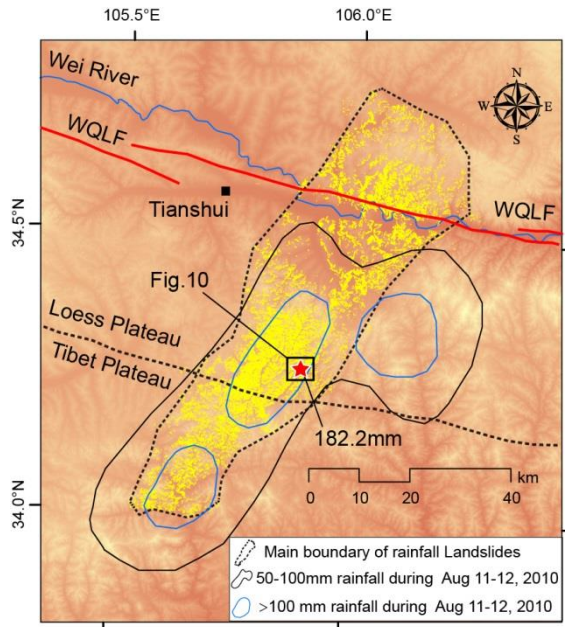
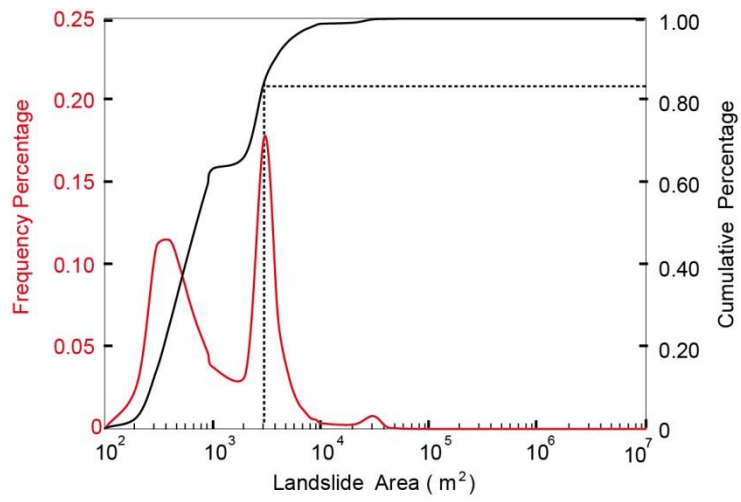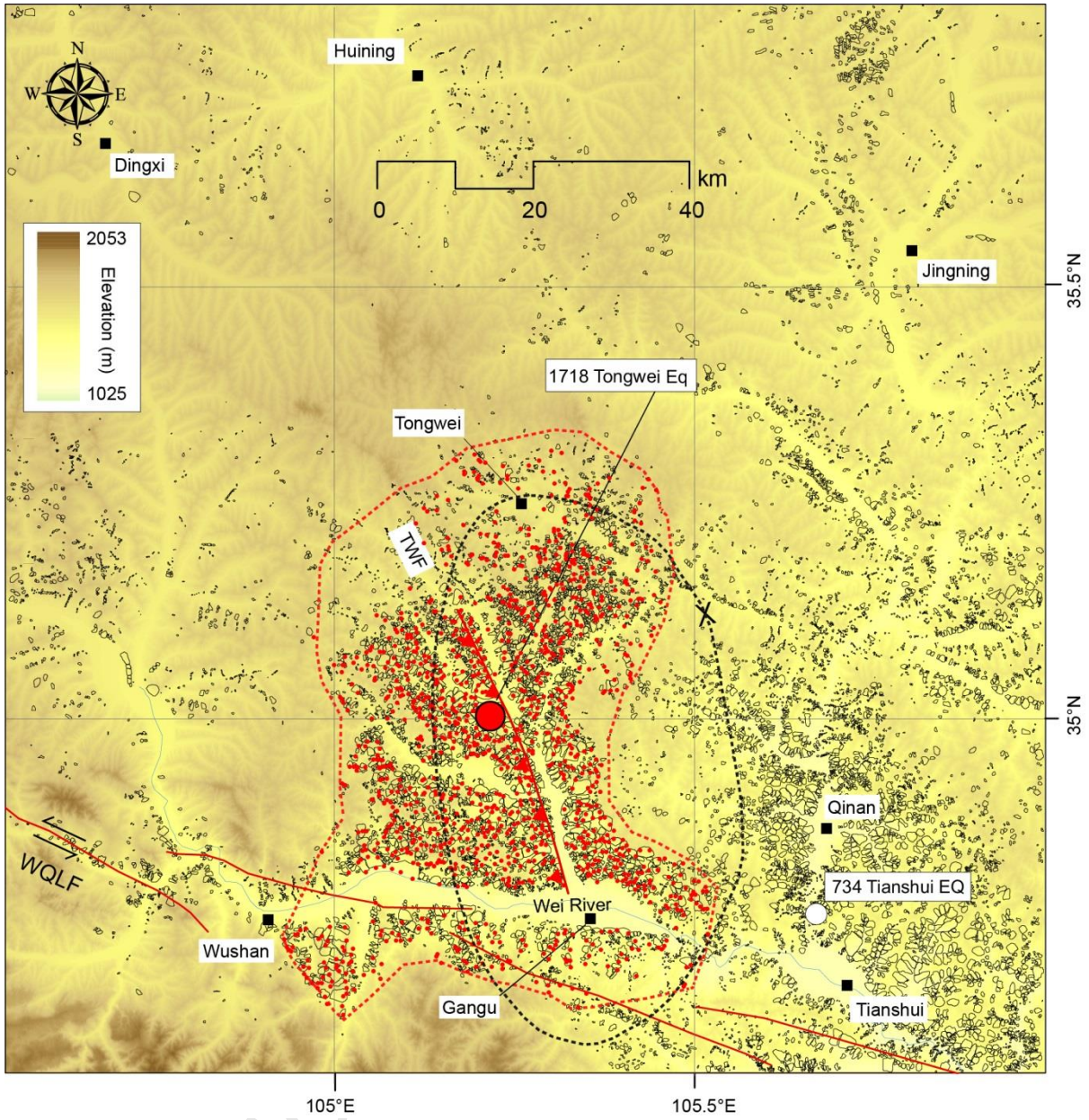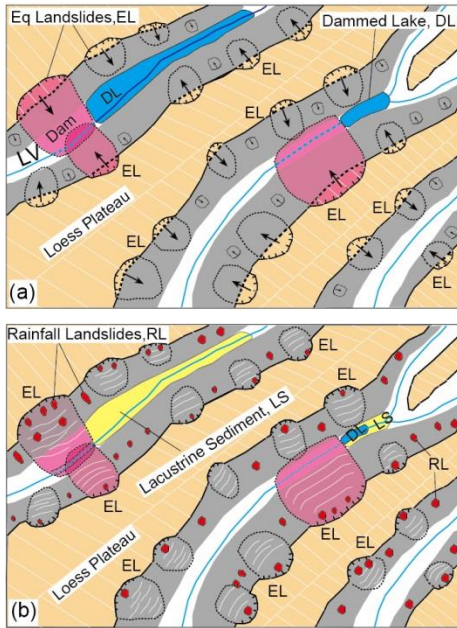**Fig.10**

Fig.11

Fig.12

Fig.13

Declaration of interests

☒ The authors declare that they have no known competing financial interests or personal relationships that could have appeared to influence the work reported in this paper.

☐The authors declare the following financial interests/personal relationships which may be considered as potential competing interests:

Highlights

- Analysis of 80,000 landslides in the Loess Plateau.

- Storms generate surficial soil landslides, easy to recover; historical earthquakes trigger both soil landslides and larger, deeper ones, only the latter can be interpreted.

- Future M >7 earthquakes may trigger landslides that could directly hit 30-50% of the communities in the epicentral area.